

ADAPTIVE TIMESTEPPING STRATEGIES FOR NONLINEAR STOCHASTIC SYSTEMS*

CÓNALL KELLY [†] AND GABRIEL J. LORD [‡]

Abstract. We introduce a class of adaptive timestepping strategies for stochastic differential equations with non-Lipschitz drift coefficients. These strategies work by controlling potential unbounded growth in solutions of a numerical scheme due to the drift. We prove that the Euler-Maruyama scheme with an adaptive timestepping strategy in this class is strongly convergent. Specific strategies falling into this class are presented and demonstrated on a selection of numerical test problems. We observe that this approach is broadly applicable, can provide more dynamically accurate solutions than a drift-tamed scheme with fixed stepsize, and can improve MLMC simulations.

Key words. Stochastic differential equations, Adaptive timestepping, Euler-Maruyama method, Locally Lipschitz drift coefficient, Strong convergence.

AMS subject classifications. 65C20, 65C30, 65L20, 65L50

1. Introduction. We investigate adaptive timestepping for the numerical approximation of a d -dimensional stochastic differential equation (SDE) of Itô type

$$(1) \quad \begin{aligned} dX(t) &= f(X(t))dt + g(X(t))dW(t), \quad t > 0, \\ X(0) &\in \mathbb{R}^d, \end{aligned}$$

where W is an m -dimensional Wiener process and the drift coefficient f is not globally Lipschitz continuous, but rather satisfies a one-sided Lipschitz condition and a polynomial growth condition.

Since it was pointed out in [13] that the Euler-Maruyama method fails to converge in the strong sense for such equations, there has been much interest in tamed numerical methods, the first of which was presented in [14] (see (8) in Section 1.1). We also refer the reader to the variant presented in [20], and to the related class of truncated methods which may be found in, for example, [19]. Generally, speaking, these methods work by enforcing a higher order modification to the drift and (if necessary) diffusion coefficients in order to control unbounded growth permitted by non-globally Lipschitz coefficients. The idea has been extended to higher order schemes [25], to SDEs with Lévy noise [6], and to stochastic partial differential equations (SPDEs) [9].

However, as noted in [24], (fully) tamed methods can lead to dynamically inaccurate results for even moderately small step-sizes, due at least in part to the perturbation of the flow that results from modifying the coefficients. We illustrate this further in Section 3 when we show, for example, that the drift-tamed Euler-Maruyama method does not give a good approximation of the period for the stochastic Van der Pol oscillator.

In this article, we propose an alternative approach to the control of growth arising from a non globally-Lipschitz drift coefficient. Rather than modifying the drift directly, we adjust the length of the timestep taken at each iteration in order to control

*Submitted to the editors October 12, 2016.

[†]Department of Mathematics, The University of the West Indies, Mona, Kingston 7, Jamaica. (conall.kelly@uwimona.edu.jm,),

Funding: Supported by a SQuARE activity entitled “Stochastic stabilisation of limit-cycle dynamics in ecology and neuroscience” funded by the American Institute of Mathematics..

[‡]Maxwell Institute, Department of Mathematics, MACS, Heriot-Watt University, Edinburgh, EH14 4AS, UK. (g.j.lord@hw.ac.uk, www.macs.hw.ac.uk/~gabriel).

the norm of the drift response. In spirit this idea is closer to the projected Euler and Milstein methods given in [4], where solutions are prevented from leaving a ball, the radius of which is dependent on the step-size. We also point out [1], where adaptive timestepping was used to control solution dynamics, and in particular to preserve the positivity of solutions of the numerical discretisation of nonlinear SDEs. The recent preprint of Fang & Giles [7] takes a related approach; see Remark 13 in Section 2.4 for a comparative discussion.

Otherwise, adaptive timestepping for SDEs has tended to concentrate on local error control; see for example [5, 15, 17, 21]. A serious drawback of using adaptive methods for SDEs is the potential requirement to interpolate the Brownian path in the case that a timestep is rejected. This is not necessary for the method we propose here, as long as the diffusion coefficient satisfies a global Lipschitz condition.

The structure of the article is as follows. The remainder of the introduction lays out the mathematical framework for the article, and summarises relevant results from the literature. In Section 2 we describe the Euler-type discretisation with random stepsize that forms the basis of our scheme. We demonstrate how stepsize controls can be motivated, either by ensuring that the discretised drift coefficient responds similarly to that of a scheme which is known to converge strongly (e.g. tamed Euler), or by examining the dynamics of the discrete drift map. Finally, we define a class of admissible timestepping strategies for (1), provide examples, and state the strong convergence theorem that is our main result.

In Section 3 we investigate our methods with two adaptive timestepping strategies and compare their performance to a tamed Euler method with fixed stepsize for eight test problems, illustrating convergence and reporting the details of stepsizes chosen by each strategy. In particular for the stochastic Van der Pol oscillator we see that the fixed-step tamed Euler method consistently underestimates the period but that adaptive methods give a better approximation. We also examine a multi-level Monte Carlo (MLMC) approximation with adaptive timestepping and observe that this approach reduces the variance on each level, leading to fewer realisations and hence reducing the computational cost. In Section 4 we provide the proof of our main result. Our conclusions and a short discussion of possible future directions for this work are in Section 5.

1.1. Mathematical preliminaries. Consider the d -dimensional Itô-type SDE (1). For the remainder of the article we let $(\mathcal{F}_t)_{t \geq 0}$ be the natural filtration of W . Suppose $f : \mathbb{R}^d \rightarrow \mathbb{R}^d$ is continuously differentiable with derivative that grows at most polynomially: for some $c \in (0, \infty)$

$$(2) \quad \|Df(x)\| \leq c(1 + \|x\|^c);$$

and satisfies a one-sided Lipschitz condition with constant $\alpha > 0$:

$$(3) \quad \langle f(x) - f(y), x - y \rangle \leq \alpha \|x - y\|^2.$$

Suppose also that $g : \mathbb{R}^d \rightarrow \mathbb{R}^{d \times m}$ is continuously differentiable and satisfies a global Lipschitz condition with constant $\kappa > 0$:

$$(4) \quad \|g(x) - g(y)\|_F \leq \kappa \|x - y\|.$$

Under conditions (2)–(4), (1) has a unique strong solution on any interval $[0, T]$, where $T < \infty$ on the filtered probability space $(\Omega, \mathcal{F}, (\mathcal{F}_t)_{t \geq 0}, \mathbb{P})$. Moreover the following moment bounds apply over any finite interval $[0, T]$:

LEMMA 1. *Let f, g be C^1 functions satisfying (3) and (4) respectively. Then for each $p > 0$ there is $C = C(p, T, X(0)) > 0$ such that*

$$(5) \quad \mathbb{E} \left[\sup_{s \in [0, T]} \|X(s)\|^p \right] \leq C.$$

This was proved as Lemma 3.2 in [10] for $p > 2$, which can be extended to include $0 < p \leq 2$ via Jensen's inequality.

The following bound is used to develop timestepping strategies in Section 2.4, and in the proof of our main theorem.

LEMMA 2. *The polynomial bound on the derivative of f given by (2) implies*

$$(6) \quad \|f(x)\| \leq c_1 \left(1 + \|x\|^{(c+1)} \right).$$

where $c_1 := 2c + \|f(0)\|$.

Proof. See, for example, Lemma 3.1 in [14]. □

The Euler-Maruyama numerical method and the notion of strong convergence may be expressed as follows.

DEFINITION 3. *Fix $T < \infty$ and $N \in \mathbb{N}$, and define $h = T/N$. The Euler-Maruyama discretisation of (1) over the interval $[0, T]$ with N steps is given by*

$$(7) \quad \begin{aligned} X_{n+1}^N &= X_n^N + hf(X_n^N) + g(X_n^N)(W((n+1)h) - W(nh)), \quad n = 0, \dots, N, \\ X_0 &= X(0). \end{aligned}$$

DEFINITION 4. *If there exists $p \in [1, \infty)$ and constants $C_p, \beta > 0$ such that*

$$(\mathbb{E} [\|X(T) - X_N^N\|^p])^{1/p} \leq C_p h^\beta,$$

then the Euler-Maruyama method given by (7) is said to converge strongly with order β in \mathcal{L}_p to solutions of (1) over the interval $[0, T]$.

In the scalar single noise case, Hutzenthaler & Jentzen [13, Theorem 1], showed that the Euler-Maruyama method given in (7) cannot converge strongly if at least one of the coefficients grows superlinearly. We restate their result here:

THEOREM 5. *Let $d = m = 1$, and let $C \geq 1$, $\beta > \alpha > 1$ be constants such that*

$$\max \{|f(x)|, |g(x)|\} \geq \frac{|x|^\beta}{C} \quad \text{and} \quad \min \{|f(x)|, |g(x)|\} \leq C|x|^\alpha$$

for all $|x| \geq C$. If the exact solution of (1) satisfies $\mathbb{E}[|X(T)|^p] < \infty$ for some $p \in [1, \infty)$, then

$$\lim_{N \rightarrow \infty} \mathbb{E} [|X(T) - X_N^N|^p] = \infty \quad \text{and} \quad \lim_{N \rightarrow \infty} |\mathbb{E} [|X(T)|^p] - \mathbb{E} [|X_N^N|^p]| = \infty.$$

The drift-tamed Euler-Maruyama method given by

$$(8) \quad Y_{n+1}^N = Y_n^N + \frac{hf(Y_n^N)}{1 + h\|f(Y_n^N)\|} + g(Y_n^N)(W((n+1)h) - W(nh)), \quad n = 0, \dots, N,$$

was introduced in [14] to provide an explicit numerical method that would display strong convergence in circumstances where the Euler-Maruyama method does not. In fact, strong convergence was proved under Conditions (2)–(4). The following theorem states two key results from that article: the first on boundedness of moments, the second on strong convergence.

THEOREM 6. [14] *Let $X(t)$ be a solution of (1), where f and g satisfy Conditions (2)–(4). Let $\{Y_n^N\}$ be a solution of (8). Then*

$$(9) \quad \sup_{n \in \mathbb{N}} \sup_{n \in \{0, 1, \dots, N\}} \mathbb{E}[\|Y_n^N\|^p] < \infty.$$

Let $\{\bar{Y}^N\}$ be a sequence of continuous time interpolants of the time discrete approximation (8). There exists a family C_p , $p \in [1, \infty)$ of real numbers such that

$$\left(\mathbb{E} \left[\sup_{t \in [0, T]} \|X(t) - \bar{Y}_t^N\|^p \right] \right)^{1/p} \leq C_p h^{1/2},$$

for all $N \in \mathbb{N}$ and all $p \in [1, \infty)$.

Higham, Mao & Stuart [10] showed that the Euler-Maruyama scheme (7) is strongly convergent in the sense of Definition 4 if its moments are bounded in the sense of (9) in the statement of Theorem 6. In Section 2 we show how stepsize control can be used to bound the drift response pathwise, sufficient to ensure strong convergence.

2. Adaptive timestepping strategies.

2.1. Euler-type schemes with random timesteps. Consider the following Euler-type method for (1) over a random mesh $\{t_n\}_{n \in \mathbb{N}}$ on the interval $[0, T]$ given by

$$(10) \quad Y_{n+1} = Y_n + h_{n+1}f(Y_n) + g(Y_n)(W(t_{n+1}) - W(t_n)), \quad Y_0 = X_0, \quad n < N,$$

where $\{h_n\}_{n \in \mathbb{N}}$ is a sequence of random timesteps, and $\{t_n := \sum_{i=1}^n h_i\}_{n=1}^N$ with $t_0 = 0$. The random time steps h_{n+1} (and the corresponding point on the random mesh t_{n+1}) are to be determined by the value of Y_n .

DEFINITION 7. *Suppose that each member of the sequence $\{t_n\}_{n \in \mathbb{N}}$ is an (\mathcal{F}_t) -stopping time: i.e. $\{t_n \leq t\} \in \mathcal{F}_t$ for all $t \geq 0$, where $(\mathcal{F}_t)_{t \geq 0}$ is the natural filtration of W . We may then define a discrete-time filtration $\{\mathcal{F}_{t_n}\}_{n \in \mathbb{N}}$ by*

$$\mathcal{F}_{t_n} = \{A \in \mathcal{F} : A \cap \{t_n \leq t\} \in \mathcal{F}_t\}, \quad n \in \mathbb{N}.$$

ASSUMPTION 8. *Suppose that each h_n is $\mathcal{F}_{t_{n-1}}$ -measurable, let N be a random integer such that*

$$N := \max\{n \in \mathbb{N} : t_{n-1} < T\} \quad \text{and} \quad t_N = T.$$

In addition let h_n satisfy the following constraint: minimum and maximum stepsizes h_{\min} and h_{\max} are imposed in a fixed ratio $0 < \rho \in \mathbb{R}$ so that

$$(11) \quad h_{\max} = \rho h_{\min}.$$

In Assumption 8, the lower bound h_{\min} ensures that a simulation over the interval $[0, T]$ can be completed in a finite number of timesteps. In the event that at time t_n we compute $h_{n+1} = h_{\min}$, we apply a single step of the drift-tamed Euler method (8) over a timestep of length $h = h_{\min}$, rather than (10). Therefore the adaptive timestepping scheme under investigation in this article is

$$(12) \quad Y_{n+1} = Y_n + h_{n+1} \left[f(Y_n) \mathcal{I}_{\{h_{n+1} > h_{\min}\}} + \frac{f(Y_n)}{1 + h_{\min} \|f(Y_n)\|} \mathcal{I}_{\{h_{n+1} = h_{\min}\}} \right] \\ + g(Y_n)(W(t_{n+1}) - W(t_n)), \quad n = 0, \dots, N-1.$$

The upper bound h_{\max} prevents stepsizes from becoming too large and allows us to examine the strong convergence of the adaptive method (12) to solutions of (1) as $h_{\max} \rightarrow 0$ (and hence as $h_{\min} \rightarrow 0$).

REMARK 9. In (12), note that each $W(t_{n+1}) - W(t_n)$ is a Wiener increment taken over a random step of length h_{n+1} which itself may depend on Y_n , and therefore is not necessarily normally distributed. However, if h_{n+1} is an \mathcal{F}_{t_n} -stopping time then $W(t_{n+1}) - W(t_n)$ is \mathcal{F}_{t_n} -conditionally normally distributed with, almost surely (a.s.),

$$\mathbb{E} \left[\|W(t_{n+1}) - W(t_n)\| \middle| \mathcal{F}_{t_n} \right] = 0, \quad \mathbb{E} \left[\|W(t_{n+1}) - W(t_n)\|^2 \middle| \mathcal{F}_{t_n} \right] = h_{n+1}.$$

In practice therefore, we can replace the sequence of Wiener increments with i.i.d. $\mathcal{N}(0, 1)$ random variables denoted $\{\xi_n\}_{n=1}^N$, scaled at each step by the \mathcal{F}_{t_n} -measurable random variable $\sqrt{h_{n+1}}$.

In Sections 2.2 and 2.3 we provide two motivating discussions, each illustrating how a timestepping strategy can be designed. The first focuses on the properties of the drift-tamed Euler method (8), the second on the local dynamics of polynomial maps. In Section 2.4 we set out a sufficient set of conditions for such strategies to ensure that solutions of (12) converge strongly to those of (1).

2.2. Stepsize selection via the drift-tamed Euler map. For the stochastic differential equation (1) the explicit Euler and drift-tamed Euler maps associated with the drift coefficient f are

$$F_h(y) = y + hf(y) \quad \text{and} \quad \tilde{F}_h(y) = y + \frac{hf(y)}{1 + h\|f(y)\|}$$

respectively. At each timestep we choose $h(y)$ so that

$$(13) \quad \|F_h(y) - \tilde{F}_h(y)\| = \frac{h^2\|f(y)\|^2}{1 + h\|f(y)\|} < \varepsilon$$

for some tolerance $\varepsilon > 0$. Equivalently we have $h^2\|f(y)\|^2 - \varepsilon h\|f(y)\| - \varepsilon < 0$ and so require h such that

$$\frac{\varepsilon - \sqrt{\varepsilon^2 + 4\varepsilon}}{2\|f(y)\|} < h < \frac{\varepsilon + \sqrt{\varepsilon^2 + 4\varepsilon}}{2\|f(y)\|}.$$

Since $\varepsilon - \sqrt{\varepsilon^2 + 4\varepsilon} < 0$ for all $\varepsilon > 0$ we are left with the requirement that

$$0 < h < \frac{1}{\|f(y)\|} \left[\frac{\varepsilon + \sqrt{\varepsilon^2 + 4\varepsilon}}{2} \right],$$

for (13) to hold. This leads to an adaptive strategy

$$(14) \quad h_{n+1}(Y_n) = \max \left\{ h_{\min}, \min \left\{ h_{\max}, \frac{1}{\|f(Y_n)\|} \left[\frac{\varepsilon + \sqrt{\varepsilon^2 + 4\varepsilon}}{2} \right] \right\} \right\}.$$

By construction, each term in the sequence $\{h_n\}_{n \in \mathbb{N}}$ is an $\mathcal{F}_{t_{n-1}}$ -measurable random variable, and Assumption 8 holds.

2.3. Stepsize selection via local dynamics. Consider the drift coefficient function

$$(15) \quad f(x) = -\gamma x|x|^\nu, \quad x \in \mathbb{R},$$

where $\gamma, \nu > 0$. The associated Euler map with stepsize h is given by the function

$$(16) \quad F_h(x) = x - h\gamma x|x|^\nu, \quad x \in \mathbb{R}.$$

Consider the discrete-time dynamics of the map given by (16) (a more detailed analysis may be found in [2]). The difference equation

$$x_{n+1} = F_h(x_n)$$

has a stable equilibrium solution at zero and an unstable two-cycle at $\{\pm \sqrt[\nu]{2/(h\gamma)}\}$.

So the basin of attraction of the zero solution is $|x_0| < \sqrt[\nu]{2/(h\gamma)}$. For fixed γ , we can increase the size of the basin of attraction arbitrarily by choosing h sufficiently small. Moreover, the derivatives are

$$F'_h(x) = \begin{cases} 1 - h\gamma(\nu+1)x^\nu, & x \geq 0, \\ 1 + h\gamma(\nu+1)x^\nu, & x < 0, \end{cases}$$

and so outside of the basin of attraction, repeated applications of the map induce oscillations that grow rapidly at a rate determined by ν . At each iteration, a stochastic perturbation with non-compact support can move trajectories outside the basin of attraction and into a regime characterised by rapidly growing oscillation.

This suggests an adaptive timestepping strategy motivated by the control of stability. Our approach is as follows. For (1) with drift coefficient given by (15), we select each stepsize to be

$$h_{n+1} = \max \left\{ h_{\min}, \min \left\{ h_{\max}, \frac{1}{\gamma|Y_n^N|^\nu} \right\} \right\}.$$

This ensures that if the solution moves out of the basin of attraction of the unperturbed equation then the stepsize is decreased so that it is included once again.

This strategy can be extended to equations with a drift coefficient satisfying the polynomial bound

$$(17) \quad \|f(x)\| \geq \|x\|^\beta/C,$$

for $C \geq 1$, $\beta > 1$ and all $\|x\| \geq C$, by considering the basin of attraction of the Euler map corresponding to the polynomial bound on f . This suggests the following adaptation strategy:

$$(18) \quad h_{n+1} = \max \left\{ h_{\min}, \min \left\{ h_{\max}, \frac{\delta}{\|Y_n^N\|^{\beta-1}} \right\} \right\}$$

for equations with drift satisfying (17) with β an odd integer and an appropriately chosen $\delta \leq h_{\max}$. More generally, if we consider the growth over a single step of a perturbation v governed by the linear equation

$$v^{new} = (I + hDf)v \quad \text{so that} \quad h = \frac{v^{new} - v}{Df v},$$

then the following strategy is indicated: for some $\delta \leq h_{\max}$, let

$$(19) \quad h_{n+1} = \max \left\{ h_{\min}, \min \left\{ h_{\max}, \frac{\delta}{\|Df(Y_n)\|} \right\} \right\}.$$

2.4. Strong convergence of adaptive timestepping methods. We begin by defining a class of timestepping strategies that guarantee the strong convergence of solutions of (12) to solutions of (1) by ensuring that, at each step of the discretisation, the norm of the drift response has a pathwise linear bound.

DEFINITION 10. *Let $\{Y_n\}_{n \in \mathbb{N}}$ be a solution of (12) where f satisfies (2)-(3) and g satisfies (4). We say that $\{h_n\}_{n \in \mathbb{N}}$ is an admissible timestepping strategy for (12) if Assumption 8 is satisfied and there exists real non-negative constants $R_1, R_2 < \infty$ such that whenever $h_{\min} < h_n < h_{\max}$,*

$$(20) \quad \|f(Y_n)\|^2 \leq R_1 + R_2 \|Y_n\|^2, \quad n = 0, \dots, N-1.$$

In the next Lemma we provide specific examples of admissible timestepping schemes.

LEMMA 11. *Let $\{Y_n\}_{n \in \mathbb{N}}$ be a solution of (12), let $\delta \leq h_{\max}$, and let c be the constant in (6). Let $\{h_n\}_{n \in \mathbb{N}}$ be a timestepping strategy that satisfies Assumption 8. $\{h_n\}_{n \in \mathbb{N}}$ is admissible for (12) if, for each $n = 0, \dots, N-1$, one of the following holds*

- (i) $h_{n+1} \leq \delta / (\|f(Y_n)\|)$;
- (ii) $h_{n+1} \leq \delta / (1 + \|Y_n\|^{1+c})$;
- (iii) $h_{n+1} \leq \delta \|Y_n\| / (\|f(Y_n)\|)$;
- (iv) $h_{n+1} \leq \delta \|Y_n\| / (1 + \|Y_n\|^{1+c})$,

whenever $h_{\min} < h_n < h_{\max}$.

Proof. For Part (i) we can apply (11):

$$\|f(Y_n)\|^2 \leq \left(\frac{\delta}{h_{n+1}} \right)^2 \leq \frac{h_{\max}^2}{h_{\min}^2} = \rho^2,$$

and so (20) is satisfied with $R_1 = \rho^2$ and $R_2 = 0$.

For Part (ii), by (6) and (11) we have

$$\|f(Y_n)\|^2 \leq (2c + \|f(0)\|)^2 (1 + \|Y_n\|^{1+c})^2 \leq (2c + \|f(0)\|)^2 \frac{h_{\max}^2}{h_{n+1}^2} \leq (2c + \|f(0)\|)^2 \rho^2.$$

and so (20) is satisfied with $R_1 = (2c + \|f(0)\|)^2 \rho^2$ and $R_2 = 0$.

For Parts (iii) and (iv) similar arguments give the bounds $\|f(Y_n)\|^2 \leq \rho^2 \|Y_n\|^2$ and $\|f(Y_n)\|^2 \leq (2c + \|f(0)\|)^2 \rho^2 \|Y_n\|^2$ respectively, so (20) is satisfied with $R_1 = 0$, $R_2 = \rho^2$ for Part (iii), and $R_2 = (2c + \|f(0)\|)^2 \rho^2$ for Part (iv). \square

Our main result shows the strong convergence in \mathcal{L}_2 with order 1/2 of solutions of (12) to solutions of (1) when $\{h_n\}_{n \in \mathbb{N}}$ is an admissible timestepping strategy.

THEOREM 12. *Let $(X(t))_{t \in [0, T]}$ be a solution of (1) with initial value $X(0) = X_0$. Let $\{Y_n\}_{n \in \mathbb{N}}$ be a solution of (12) with initial value $Y_0 = X_0$ and admissible timestepping strategy $\{h_n\}_{n \in \mathbb{N}}$ satisfying the conditions of Definition 10. Then*

$$\left(\mathbb{E} [\|X(T) - Y_N\|^2] \right)^{1/2} \leq C h_{\max}^{1/2},$$

for some $C > 0$, independent of h_{\max} .

The proof of Theorem 12 is a modification of a standard Euler-Maruyama convergence argument accounting for the properties of the random sequences $\{t_n\}_{n \in \mathbb{N}}$ and $\{h_n\}_{n \in \mathbb{N}}$, and using (20) to compensate for the non-Lipschitz drift. It is presented in Section 4.

It is possible to link the notion of admissibility to the strategies developed via taming and local dynamics in Sections 2.2 and 2.3 as follows. The adaptive timestepping strategy given by (14) is admissible for an appropriate choice of tolerance ε : to

see this, let

$$0 \leq \varepsilon < \frac{h_{\max}^2}{1 + h_{\max}}.$$

Then (14) is equivalent to the strategy given in Part (i) of Lemma 11, with

$$\delta := \frac{\varepsilon + \sqrt{\varepsilon^2 + 4\varepsilon}}{2} \leq h_{\max}.$$

We investigate performance of (14) numerically in Section 3.

The adaptive timestepping strategy given by (18) in Section 2.3 is equivalent to that given in Part (iii) of Lemma 11 when the drift coefficient is precisely the polynomial expression on the right hand side of (17), and (18) is therefore admissible in that case. For more general drift coefficients the closest correspondence is with Part (iv) of Lemma 11, for which a priori knowledge of the polynomial bound parameter c is needed; in practice this may be difficult to determine. The variant given by (19), which uses the norm of the Jacobian of f , is not known to be admissible but neither does it require precise knowledge of c , and we investigate it numerically in Section 3.

REMARK 13. In [7], an adaptive timestepping strategy is presented which satisfies

$$(21) \quad \langle Y_n, f(Y_n) \rangle + \frac{1}{2} h_{n+1} \|f(Y_n)\|^2 \leq \alpha \|Y_n\|^2 + \beta, \quad n = 0, \dots, N-1,$$

where the one sided linear bound $\langle x, f(x) \rangle \leq \alpha \|x\|^2 + \beta$, for $\alpha, \beta > 0$, has been imposed upon the drift coefficient f . With additional upper and lower bounds on each timestep, and the introduction of a convergence parameter $\delta \leq 1$, the authors show that the Euler-Maruyama scheme is strongly convergent with order 1/2.

We note that, in Section 3.1 of [7], specific timestepping rules are proposed for two scalar equations with drift satisfying a polynomial bound of the form (17) for large arguments: the stochastic Ginzburg Landau equation and the stochastic Verhulst equation. These rules are consistent with the adaptive timestepping strategy given by (18). Similarly, in Section 3.2, two specific timestepping rules for multi-dimensional SDEs are proposed, the first of which, within our framework, corresponds to Part (iii) of Lemma 11. The second of those rules, within our framework, corresponds to

$$h_{n+1} \leq \delta \frac{\|Y_n\|^2}{\|f(Y_n)\|^2}.$$

If we suppose that $\delta \leq h_{\max}$ then we have

$$\|f(Y_n)\|^2 \leq \frac{\delta}{h_{n+1}} \|Y_n\|^2 \leq \rho \|Y_n\|^2,$$

which is admissible for (12).

3. Numerical examples. In the numerical experiments below we compare two different adaptive time-stepping strategies for (12) with the fixed step drift-tamed Euler-Maruyama scheme (8). For the latter we take as the fixed step h_{mean} the average of all timesteps $h_n^{(m)}$ over each path and each realisation $m = 0, 1, \dots, M$ so that

$$h_{\text{mean}} = \frac{1}{M} \sum_{m=1}^M \frac{1}{N^{(m)}} \sum_{n=1}^{N^{(m)}} h_n^{(m)}.$$

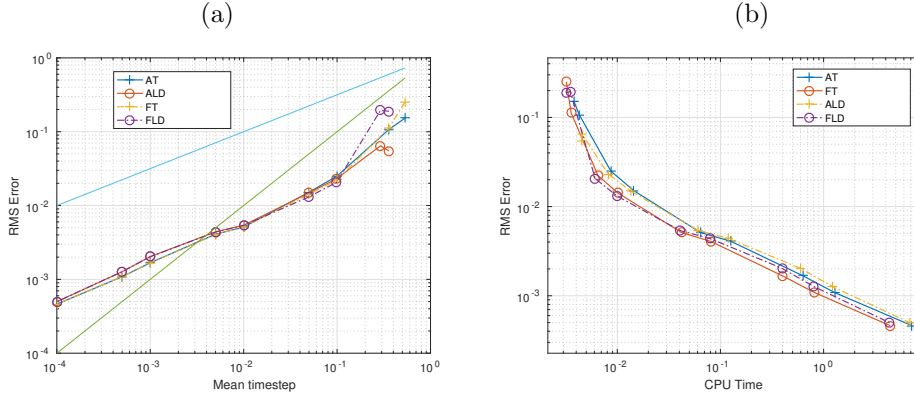


FIG. 1. **(a)**: A numerical demonstration of strong convergence for multiplicative noise as the mean stepsize decreases for the adaptive methods AT, ALD and fixed step methods FT, FLD applied to Eq. (22) with parameters $\eta = 0.1$, $\lambda = 2$ and $\sigma = 0.5$. $T = 2$. **(b)** plot showing the efficiency and reduction in root mean square (RMS) error as the CPU time (s) increases and h_{\max} decreases. For each h_{\max} value $\rho = 100$.

Thus we are comparing to a fixed step scheme of similar average cost. We solve (12) with the taming inspired adaptive timestepping strategy (14) and denote this AT. The fixed step comparison using h_{mean} computed from AT is denoted FT. Similarly, we solve (12) with the local dynamics inspired adaptive timestepping scheme (19) which we denote ALD and the fixed step comparison is denoted FLD.

3.1. A stochastic Ginzburg Landau equation. This equation arises from the theory of superconductivity and takes the form

$$(22) \quad dX(t) = \left(\left(\eta + \frac{1}{2}\sigma^2 \right) X(t) - \lambda X(t)^3 \right) dt + \sigma G(X(t)) dW(t), \quad X(0) = x_0 > 0,$$

for $t \geq 0$, and where $\eta \geq 0$ and $\lambda, \sigma > 0$. When $G(X) = X$, the explicit form of the solution over $[0, \infty)$, provided by Kloeden & Platen [16], is

$$(23) \quad X(t) = \frac{x_0 \exp(\eta t + \sigma W(t))}{\sqrt{1 + 2x_0^2 \lambda \int_0^t \exp(2\eta s + 2\sigma W(s)) ds}}, \quad t \geq 0.$$

We use this exact solution to illustrate numerically the strong convergence result of Theorem 12, see Figure 1, computing to a final time of $T = 2$ with 100 realisations. We compare in Figure 1 (a) all four methods AT, FT, ALD and FLD and show reference lines of slope 1 and 1/2. Note that the global error of the adaptive methods at time T is close to that computed with the mean step h_{mean} by the fixed step method. In (b) we show comparison of estimated rates of strong convergence and root mean square error (RMS) error against the CPU time between the adaptive methods AT, ALD and the fixed step tamed Euler methods FT, FLD. We see there is a slight computational overhead in performing the adaptive step which is expected. In Figure 2 we examine convergence for (22) with additive noise (taking $G(X) = 1$). As we do not have an exact solution we use a reference solution computed with $h = 10^{-5}$ using (8). We observe, as for a standard Euler-Maruyama method, an improvement in the rate of convergence for the adaptive methods AT, ALD as well as the fixed step schemes FT and FLD. Comparing with h_{mean} leads to similar errors and we again note a slight computational overhead to account for the adaptive step in the algorithm.

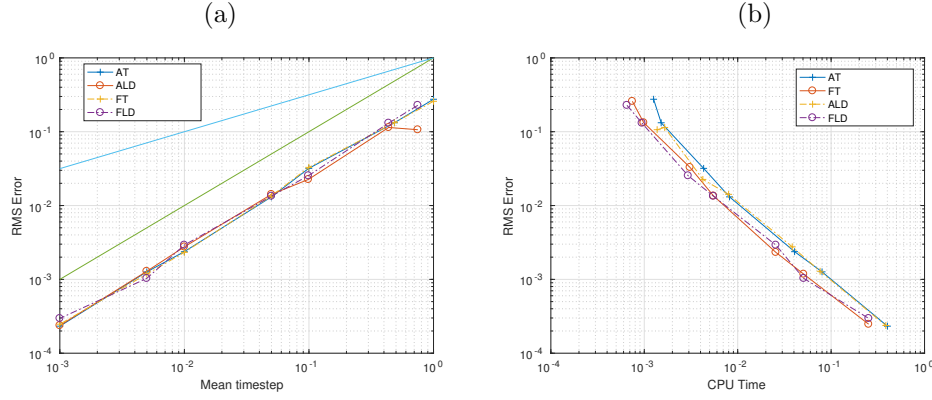


FIG. 2. (a): A numerical demonstration of strong convergence for additive noise as the mean stepsize decreases for the adaptive methods AT, ALD and fixed step methods FT, FLD applied to Eq. (22) with parameters $\eta = 0.1$, $\lambda = 2$ and $\sigma = 0.5$. $T = 2$. (b) plot showing the efficiency and reduction in root mean square (RMS) error as the CPU time (s) increases and h_{\max} decreases. For each h_{\max} value $\rho = 100$.

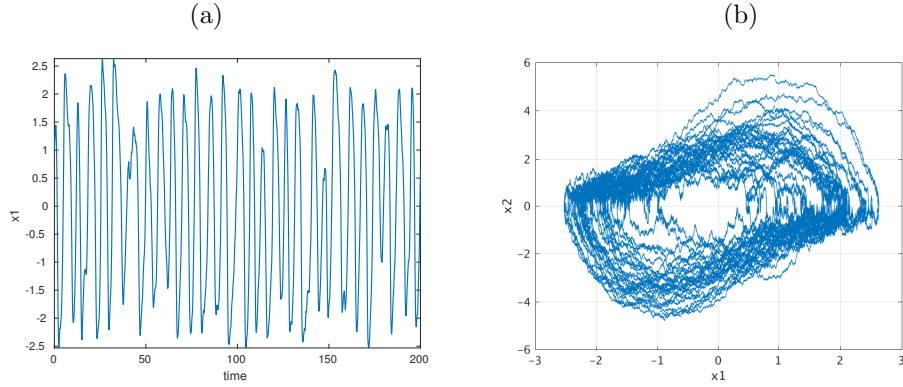


FIG. 3. A single realisation of (24) obtained using (8) with $h = 10^{-4}$. (a) shows $X_1(t)$ against time and (b) the phase portrait.

3.2. The stochastic Van der Pol oscillator. This is a stochastic additive noise version of the van der Pol oscillator, which describes the effect of external noise on stable oscillations, and takes the form

$$(24) \quad d \begin{pmatrix} X_1(t) \\ X_2(t) \end{pmatrix} = \begin{pmatrix} X_2(t) \\ (1 - (X_1(t))^2)X_2(t) - X_1(t) \end{pmatrix} dt + \begin{pmatrix} 0 \\ dW(t) \end{pmatrix}.$$

In Figure 3 we show two realisations for (24) obtained using the drift-tamed Euler–Maruyama scheme (8) with $h = 10^{-4}$. We clearly see periodic behaviour over the interval $[0, T]$. We ask how well the period is captured by the adaptive methods AT and ALD and by the fixed step methods FT and FLD. Figure 4 compares two realisations computed using the same paths for $W(t)$, so that the path in (a) is the same as that in (b) (similarly for (c) and (d)). We observe that the fixed step methods FT and FLD in (b) and (d) appear to have fewer oscillations than the adaptive simulations in (a) and (c) (and Figure 3 (a)).

This is borne out in Table 1 which compares data on the estimated mean period

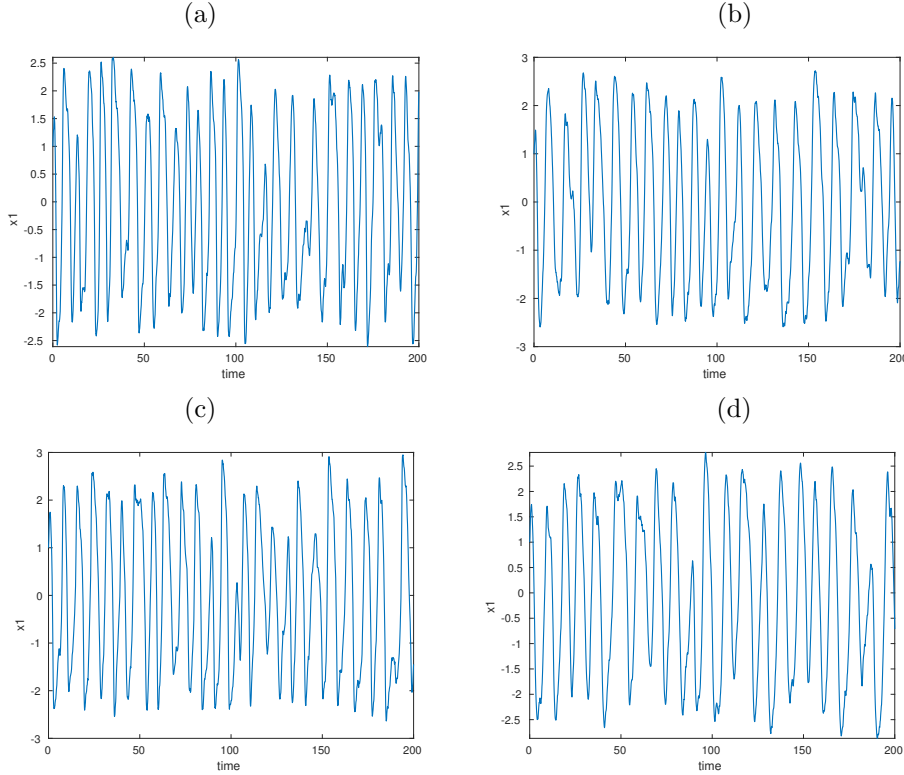


FIG. 4. Sample realisations to (24) obtained using AT (a) compared to $h = 0.0838$ for FT in (b). In (c) we use ALD and compare to FLD with $h = 0.1269$ in (d). Here $\rho = 100$ and $h_{\max} = 1$. Note that the paths in (a) and (b) (and (c) and (d)) are the same and the difference arises from the timestepping.

	Rel. Error	Mean Period	Var	Min	Max	h
TE (8)		6.684832	0.294930	5.555556	9.090909	0.0005
AT	0.089037	7.355539	0.484346	5.882353	9.090909	
FT	0.213953	8.543185	0.808813	7.142857	11.111111	0.080635
TE (8)		6.725343	0.250395	5.555556	8.333333	0.0005
ALD	0.183946	8.368017	1.750757	6.250000	14.285714	
FLD	0.279599	9.394958	1.132636	7.142857	14.285714	0.120965

TABLE 1

Comparison for the van der Pol equation (24) of estimated mean period, variance, minimum period and maximum period based on 100 realisations with $\rho = 100$, $h_{\max} = 1$ and $T = 100$. We also report an estimate of the relative error in the mean period.

and variance from 100 realisations of (24) for $t \in [0, 100]$. We also include maximum and minimum periods observed. The adaptive methods AT and ALD both give a better estimate of the period than the equivalent fixed step methods and have a smaller relative error. We also note that AT uses, on average, smaller steps than ALD and has a smaller relative error. For the equivalent fixed step schemes FT and FLD the error for these different timesteps are similar.

In Table 2 we examine for $T = 200$ the timesteps h_n taken by AT and ALD

	ρ	h_{mean}	$\text{Var } h_n^{(m)}$	$\text{Min } h_n^{(m)}$	$\text{Max } h_n^{(m)}$	cpu (s)	% Min
AT	1000	0.080644	0.004299	0.012224	0.823429	1.068599	0.000000
AT	100	0.081051	0.004195	0.020000	0.798538	1.071684	6.064423
AT	10	0.207301	0.001526	0.200000	0.820070	0.461500	89.625417
ALD	1000	0.122547	0.008976	0.022985	0.499999	0.663723	0.000000
ALD	100	0.121729	0.008901	0.023002	0.499999	0.671226	0.087541
ALD	10	0.220997	0.004053	0.200000	0.499998	0.413096	83.616568

TABLE 2

Comparison of step size data h_n for the stochastic Van der Pol equation (24) with additive noise based on 100 realisations. See Table 3 for an example with multiplicative noise.

	ρ	h_{mean}	$\text{Var } h_n^{(m)}$	$\text{Min } h_n^{(m)}$	$\text{Max } h_n^{(m)}$	cpu	% Min
AT	1000	0.084782	0.025490	0.011188	1.487107	0.104582	0.000000
AT	100	0.085909	0.024528	0.020000	1.396040	0.114417	19.373834
AT	10	0.237467	0.023662	0.200000	1.118137	0.040255	87.013139
ALD	1000	0.012929	0.001416	0.002009	0.464278	0.790780	12.960151
ALD	100	0.035592	0.003088	0.020000	0.468432	0.288227	74.265358
ALD	10	0.212098	0.002462	0.200000	0.446987	0.046083	93.070037

TABLE 3

Comparison of step size data h_n for the Langevin equation (25) with multiplicative noise based on 100 realisations. See Table 2 for an example with additive noise.

for different values of ρ with $h_{\text{max}} = 2$. We report h_{mean} , along with the timestep variance, the minimum and maximum timesteps, the computational time taken, and the percentage of timesteps taken at the minimum h_{min} . We see that for ρ large enough h_{min} is not reached often and the frequency with which this occurs for $\rho = 100$ (where $h_{\text{min}} = 0.02$) is similar to that for $\rho = 1000$ (where $h_{\text{min}} = 0.002$).

3.3. A Langevin equation. The following example is taken from [17]:

$$\begin{aligned}
 dX_1(t) &= X_2(t)dt \\
 (25) \quad dX_2(t) &= - \left[\frac{1}{2} X_2(t) \left(\frac{4(5X_1(t)^2 + 1)}{5(X_1(t)^2 + 1)} \right)^2 \right] dt + \frac{4(5X_1(t)^2 + 1)}{5(X_1(t)^2 + 1)} dW(t).
 \end{aligned}$$

We take $X(0) = [1, 1]^T$ and solve to $T = 20$ with $h_{\text{max}} = 2$. We now examine the choice of ρ . In Table 3 we give the mean step h_{mean} , variance, minimum and maximum step, computational time and the percentage of steps that were at h_{min} . Note that both h_{max} and h_{mean} is larger for AT than ALD (and we see a smaller computational time). In Figure 5 we plot the percentage of the number of steps taken at the minimum step size as ρ is increased for AT and ALD. We see that for small ρ the minimum step h_{min} is reached with a high probability (1 when $\rho = 1$). As ρ is increased for both schemes the minimum step is no longer reached (at $\rho = 10^3$ for (19) and $\rho = 10^4$ for (13)). This illustrates that the time adaptivity is actively controlling the dynamics (and we are not at the minimum step at each iteration). Although from Figure 5 we can not see that AT or ALD takes larger or smaller steps we can see that the step size choice is different and that the variance is smaller for ALD (and in some situations it may be preferable not to have large switches in stepsize).

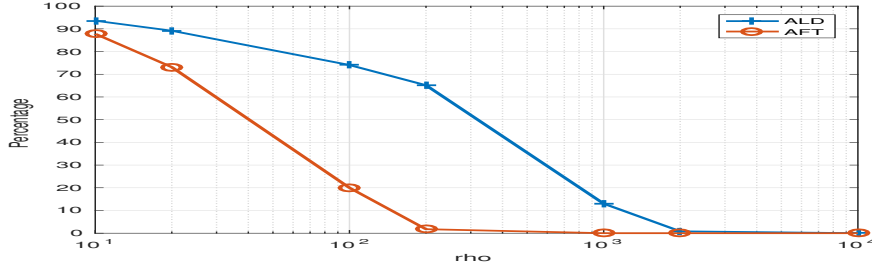


FIG. 5. As ρ increases, the percentage of steps taken at the smallest step h_{\min} decreases for AT and ALD. Here $h_{\max} = 2$ and so $h_{\min} = 0.2, \dots, 0.0002$.

3.4. Comparison of step sizes for 8 different problems. Both AT and ALD control growth from a non globally Lipschitz drift term. We now compare the timestep selection made by each of these over a range of different problems. Rather than present tables on data such as in Table 2 or 3 we summarize the mean and variance in Figure 6 for $\rho = 100$ (a) and $\rho = 1000$ in (b). We include the stochastic Van der Pol oscillator (24) (VdP), the Langevin equation (25) (Lang), and the Stochastic Ginzburg-Landau equation (22) with $G(X) = 1$ (additive noise) (SGLA). The other models that we examine can also be found, for example, in [12]. Note that for certain of these models the coefficients change randomly on each realisation.

SIR: Simulation of the stochastic Susceptible, Infected, Recovered (SIR) model

$$\begin{aligned} dX_1(t) &= [-\alpha X_1(t)X_2(t) - \delta X_1(t) + \delta]dt + [-\beta X_1(t)X_2(t)]dW_1(t), \\ dX_2(t) &= [\alpha X_1(t)X_2(t) - (\gamma + \delta)X_2(t)]dt + [\beta X_1(t)X_2(t)]dW_2(t), \\ dX_3(t) &= [\gamma X_2(t) - \delta X_3(t)]dt, \end{aligned}$$

over the simulation interval $[0, T]$, $T = 2$ with initial data $X(0) = [0.5; 0.3; 0.2]$.

For each simulation we take $\alpha, \beta, \gamma, \delta \sim U[0, 10]$.

LV: Simulation of the stochastic Lotka-Volterra (LV) model in the well stirred sense

$$\begin{aligned} dX_1(t) &= [X_1(t)(\alpha - \beta X_2(t))]dt + \sigma_1 X_1(t)dW_1(t), \\ dX_2(t) &= [X_2(t)(\gamma X_1(t) - \delta)]dt + \sigma_2 X_2(t)dW_2(t), \end{aligned}$$

over the simulation interval $[0, T]$ with $T = 20$ and initial value $X(0) = [5, 10]^T$. The parameters $\alpha, \beta, \gamma, \delta \sim U[0, 1]$ for each realisation and $\sigma_1 = \sigma_2 = 0.01$.

PK: Simulation of a Proto-Kinetics (PK) model. Here X represents the proportion of one form of a certain protein and therefore should be constrained to the interval $[0, 1]$ and can be modelled by the following SDE

$$\begin{aligned} dX(t) &= \left[\frac{1}{2} - X(t) + X(t)(1 - X(t)) + \frac{1}{2}X(t)(1 - X(t))(1 - 2X(t)) \right] dt \\ &\quad + [X(t)(1 - X(t))]dW(t). \end{aligned}$$

We take the simulation interval to be $[0, T]$, $T = 100$.

2D: Simulations of the polynomial type SDE

$$dX(t) = (AX(t) - \beta X(t)|X(t)|^\nu)dt + GdW(t),$$

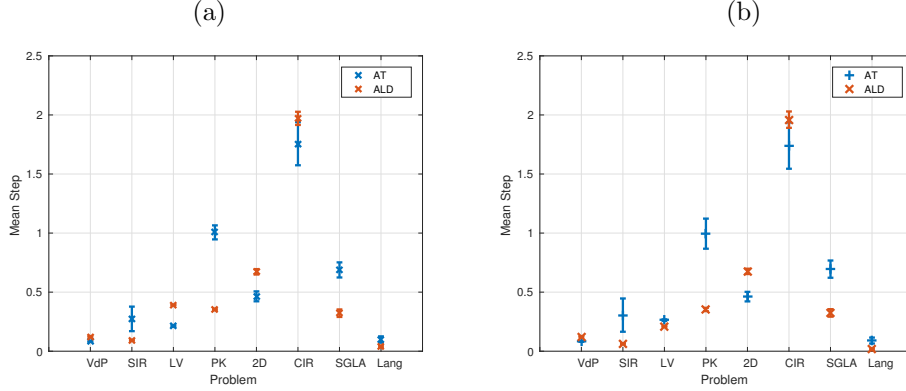


FIG. 6. Comparison of mean step sizes h_{mean} for 8 different problems with $h_{\text{max}} = 1$ (a) $\rho = 100$ and (b) $\rho = 1000$.

where $A, \beta, G \in \mathbb{R}^{J \times J}$ $X(0) = [-1; -1]^T$. We take $\nu = 2$ and

$$A = \begin{pmatrix} 0.807019 & 0.589848 \\ 0.080506 & 0.477723 \end{pmatrix}, \quad \beta = \begin{pmatrix} 0.99133 & 0.60672 \\ 0.29234 & 0.96434 \end{pmatrix}, \quad G = \begin{pmatrix} 0.5 & 0 \\ 0 & 0.5 \end{pmatrix}.$$

CIR: Simulation of special case of the stochastic Cox-Ingersoll-Ross (CIR) model

$$X(t) = \kappa(\theta - X)dt + \sigma\sqrt{X}dW, \quad X(0) = 1$$

over $[0, T]$, $T = 200$ with $\kappa = 0.1$, $\theta = 0.5$ and $\sigma = 0.5$.

3.5. Stochastic Allen-Cahn SPDE. To investigate adaptive timestepping for a large system of SDEs we consider the discretisation of the Allen-Cahn SPDE

$$du = [Du_{xx} + u - u^3] dt + \sigma dW,$$

with $x \in [0, 1]$, periodic boundary conditions, and initial data $u(0, x) = \sin(2\pi x)$. The Q -Wiener process W is white in time and takes values in $H_{\text{per}}^1(0, 1)$. We take $D = 0.01$ and $\sigma = 0.5$ and discretise in space by a spectral Galerkin approximation [18] to get an SDE system in \mathbb{R}^{100} . We take $h_{\text{max}} = 0.05$ and $\rho = 100$. We show in Figure 7 (a) the $L^2(0, 1)$ norm of one sample realisation as we solve over $t \in [0, 10]$ using AT and in (b) we plot the corresponding timestep h_n . Note that where the $L^2(0, 1)$ of the solution becomes small in (a), and hence the non-linearity becomes small, larger steps are taken.

3.6. An application to multi-level Monte-Carlo simulation. One major motivation in [13] for looking at the non-convergence of the Euler-Maruyama method was the recent interest in multi-level Monte-Carlo (MLMC) methods for SDEs, see for example [8, 18]. In its basic form the idea is to use a telescoping sum over different numerical approximations (levels) as a form of variance reduction. If we seek to estimate some (Lipschitz) quantity of interest Q of the solution $X(T)$ to the SDE we can use approximations with a hierarchy of accuracies from most accurate L to least accurate 0 and have

$$\mathbb{E}[Q(X_L)] = \mathbb{E}[Q(X_{L_0})] + \sum_{j=L_0}^{L-1} \mathbb{E}[Q(X_{j+1}) - Q(X_j)].$$

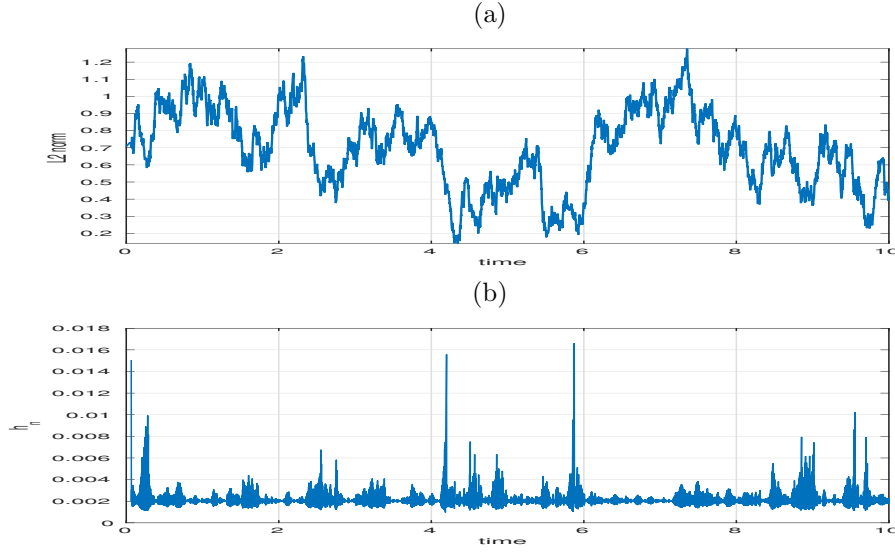


FIG. 7. (a) $L^2(0,1)$ norm of a single realisation on the stochastic Allen-Cahn SPDE solved using a spectral Galerkin system and AT. The corresponding timesteps h_n are shown in (b).

We can estimate each expectation on the right hand side with a different number of realisations determined according to the method described in [8, 18], and as j increases we would expect to take fewer realisations.

We implemented the MLMC method for AT and illustrate results below for the Stochastic Ginzburg-Landau equation with additive noise, i.e. (22) with $G(X) = 1$. In our implementation we formed each level by imposing a level dependent $h_{\max}^\ell = h_{\max}^0 k^{-\ell}$, with $h_{\max}^0 = 1$ and $k = 4$. We compare the number of realisations (and hence computational cost) to those required for the drift-tamed Euler-Maruyama method (8). We observe in Figure 8 (a) that with the adaptive timestepping the variance is reduced at each level compared to taking fixed steps and hence the number of samples required at each level is also reduced (b). This is consistent with other adaptive timestepping results [7, 11].

4. Proof of main result.

LEMMA 14. Let $(X(t))_{t \in [0, T]}$ be a solution of (1) with initial value $X(0) = X_0$, and with drift and diffusion coefficients f and g satisfying conditions (2)–(4). Let $\{t_n\}_{n \in \mathbb{N}}$ arise from an adaptive timestepping strategy for (12) satisfying the conditions of Assumption 8. Consider the Taylor expansions of f and g

$$f(X(s)) = f(X(t_n)) + R_f(s, t_n, X(t_n)), \quad g(X(s)) = g(X(t_n)) + R_g(s, t_n, X(t_n)),$$

where the remainders R_f and R_g are given in integral form by

$$R_z(s, t_n, X(t_n)) := \int_0^1 Dz(X(t_n) + \tau(X(s) - X(t_n)))(X(s) - X(t_n))d\tau,$$

and z can be taken to read either f or g . Then there are a.s. finite and \mathcal{F}_{t_n} -measurable random variables $\bar{K}_1, \bar{K}_2 > 0$, and constants $K_1, K_2, K_3 < \infty$, the latter three inde-

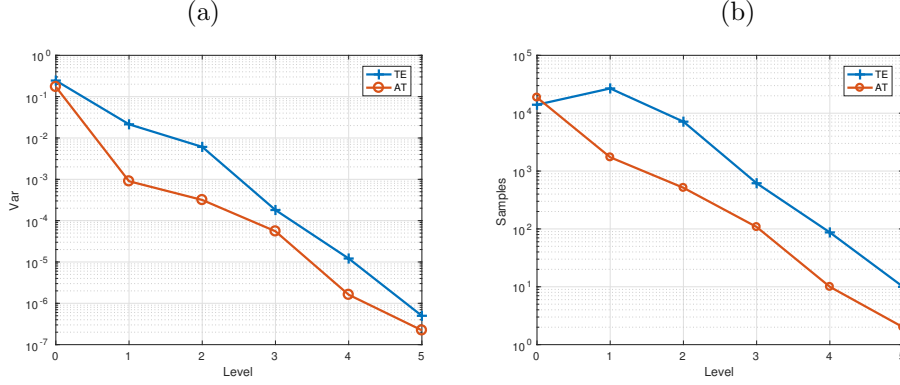


FIG. 8. Variance against level and number of samples against level for AT and (8) (a). As levels increase the variance decreases due to the strong error estimate and hence number of samples taken on each level decreases (b). We see that fewer samples are required on each level with the adaptive method AT.

pendent of h_{n+1} , such that

- (i) $\mathbb{E} \left[\left\| \int_{t_n}^{t_{n+1}} R_z(s, t_n, X(t_n)) ds \right\| \middle| \mathcal{F}_{t_n} \right] \leq \bar{K}_1 h_{n+1}^{3/2}, \quad a.s.$
- (ii) $\mathbb{E} \left[\left\| \int_{t_n}^{t_{n+1}} R_z(s, t_n, X(t_n)) ds \right\|^2 \middle| \mathcal{F}_{t_n} \right] \leq \bar{K}_2 h_{n+1}^2, \quad a.s.$
- (iii) $\mathbb{E}[\bar{K}_1] \leq K_1, \quad \text{and} \quad \mathbb{E}[\bar{K}_2] \leq K_2.$
- (iv) $\mathbb{E} \left[\bar{K}_1 \left(R_1 + 2R_2 \|X(t_n)\|^2 c_1^2 \left(1 + 2\|X(t_n)\|^{c+1} + \|X(t_n)\|^{2(c+1)} \right) \right) \right] \leq K_3.$

Proof. Let t_n be a term of $\{t_n\}_{n \in \mathbb{N}}$, and suppose that $t_n < s \leq T$. Then

$$X(s) - X(t_n) = \int_{t_n}^s f(X(r)) dr + \int_{t_n}^s g(X(r)) dW(r).$$

By the triangle inequality, Jensen's inequality, and the conditional form of the Itô isometry,

$$\begin{aligned} & \mathbb{E} [\|X(s) - X(t_n)\|^2 | \mathcal{F}_{t_n}] \\ & \leq 2\mathbb{E} \left[\left\| \int_{t_n}^s f(X(r)) dr \right\|^2 \middle| \mathcal{F}_{t_n} \right] + 2\mathbb{E} \left[\int_{t_n}^s \|g(X(r))\|_F^2 dr \middle| \mathcal{F}_{t_n} \right] \\ & \leq 2 \int_{t_n}^s \mathbb{E} [\|f(X(r))\|^2 | \mathcal{F}_{t_n}] dr + 2 \int_{t_n}^s \mathbb{E} [\|g(X(r))\|_F^2 | \mathcal{F}_{t_n}] dr, \quad a.s. \end{aligned}$$

Next, we apply (4) and (6) to get

$$\begin{aligned}
& \mathbb{E} [\|X(s) - X(t_n)\|^2 | \mathcal{F}_{t_n}] \\
& \leq 4 \int_{t_n}^s \mathbb{E} [c_1^2 (1 + \|X(r)\|^{2c+2}) | \mathcal{F}_{t_n}] dr + 2\kappa^2 \int_{t_n}^s \mathbb{E} [\|X(r)\|^2 | \mathcal{F}_{t_n}] dr \\
& \leq \left(4\mathbb{E} \left[c_1^2 \left(1 + \sup_{u \in [0, T]} \|X(u)\|^{2c+2} \right) \middle| \mathcal{F}_{t_n} \right] \right. \\
& \quad \left. + 2\kappa^2 \mathbb{E} \left[\sup_{u \in [0, T]} \|X(u)\|^2 \middle| \mathcal{F}_{t_n} \right] \right) |s - t_n| \quad a.s.
\end{aligned}$$

Therefore, by (5) in the statement of Lemma 1, we can define an a.s. finite and \mathcal{F}_{t_n} -measurable random variable

$$(26) \quad \bar{L}_n := \left(4\mathbb{E} \left[c_1^2 \left(1 + \sup_{u \in [0, T]} \|X(u)\|^{2c+2} \right) \middle| \mathcal{F}_{t_n} \right] + 2\kappa^2 \mathbb{E} \left[\sup_{u \in [0, T]} \|X(u)\|^2 \middle| \mathcal{F}_{t_n} \right] \right),$$

so that

$$(27) \quad \mathbb{E} [\|X(s) - X(t_n)\|^2 | \mathcal{F}_{t_n}] \leq \bar{L}_n |s - t_n|, \quad a.s.$$

Now consider Part (i) with R_f . By (2), and the Cauchy-Schwarz inequality

$$\begin{aligned}
& \mathbb{E} [\|R_f(s, t_n, X(t_n))\| | \mathcal{F}_{t_n}] \\
& \leq c_1 \mathbb{E} \left[\int_0^1 (1 + \|X(t_n) + \tau(X(s) - X(t_n))\|^c) \|(X(s) - X(t_n))\| d\tau \middle| \mathcal{F}_{t_n} \right] \\
& \leq c_1 \sqrt{\mathbb{E} [\|(X(s) - X(t_n))\|^2 | \mathcal{F}_{t_n}]} \\
& \quad \times \sqrt{\mathbb{E} \left[\int_0^1 (1 + \|X(t_n) + \tau(X(s) - X(t_n))\|^c)^2 d\tau \middle| \mathcal{F}_{t_n} \right]}, \quad a.s.
\end{aligned}$$

By (5) in the statement of Lemma 1 we can define an a.s. finite and \mathcal{F}_{t_n} -measurable random variable

$$\bar{M}_n := \mathbb{E} \left[2c_1^2 + 18c_1^2 \sup_{u \in [0, T]} \|X(u)\|^{2c} \middle| \mathcal{F}_{t_n} \right]$$

and so, by (27),

$$\mathbb{E} [\|R_f(s, t_n, X(t_n))\| | \mathcal{F}_{t_n}] \leq \sqrt{\bar{M}_n \bar{L}_n} \sqrt{|s - t_n|}, \quad a.s.$$

Since t_{n+1} is an \mathcal{F}_{t_n} -measurable random variable, there is an a.s. finite and \mathcal{F}_{t_n} -measurable random variable $0 < \bar{K}_1 := \frac{2}{3} \sqrt{\bar{M}_n \bar{L}_n}$ such that

$$\begin{aligned}
\mathbb{E} \left[\left\| \int_{t_n}^{t_{n+1}} R_f(s, t_n, X(t_n)) ds \right\| \middle| \mathcal{F}_{t_n} \right] & \leq \int_{t_n}^{t_{n+1}} \mathbb{E} [\|R_f(s, t_n, X(t_n))\| | \mathcal{F}_{t_n}] ds \\
& \leq \sqrt{\bar{M}_n \bar{L}_n} \int_{t_n}^{t_{n+1}} \sqrt{|s - t_n|} ds \leq \bar{K}_1 h_{n+1}^{3/2}, \quad a.s.
\end{aligned}$$

For Part (i) with R_g , the same approach using the global Lipschitz condition (4) instead of (3) yields the result.

Now consider Part (ii) with R_f . We have by (5) and the Cauchy-Schwarz inequality

$$\begin{aligned}
& \mathbb{E} \left[\left\| \int_{t_n}^{t_{n+1}} R_f(s, t_n, X(t_n)) ds \right\|^2 \middle| \mathcal{F}_{t_n} \right] \\
& \leq c \mathbb{E} \left[\left\| \int_{t_n}^{t_{n+1}} \int_0^1 Df((X(t_n) + \tau(X(s) - X(t_n)))(X(s) - X(t_n)) d\tau ds \right\|^2 \middle| \mathcal{F}_{t_n} \right] \\
& \leq c \mathbb{E} \left[\left\| \int_{t_n}^{t_{n+1}} ds \right\|^2 \right. \\
& \quad \times \left. \sup_{u \in [t_n, t_{n+1}]} \int_0^1 (1 + \|X(t_n) + \tau(X(u) - X(t_n))\|^c)^2 \|X(u) - X(t_n)\|^2 d\tau \middle| \mathcal{F}_{t_n} \right] \\
& \leq c \sqrt{\mathbb{E} \left[\left\| \int_{t_n}^{t_{n+1}} ds \right\|^4 \middle| \mathcal{F}_{t_n} \right]} \\
& \quad \times \sqrt{\mathbb{E} \left[\left(\sup_{u \in [0, T]} 4 \int_0^1 (1 + (1 + 2\tau)^c \|X(u)\|^c)^2 \|X(u)\|^2 d\tau \right)^2 \middle| \mathcal{F}_{t_n} \right]} \\
& \leq \bar{K}_2 h_{n+1}^2, \quad a.s.,
\end{aligned}$$

where \bar{K}_2 is the a.s. finite and \mathcal{F}_{t_n} -measurable random variable

$$\bar{K}_2 := \sqrt{128c^2 \mathbb{E} \left[\sup_{u \in [0, T]} (\|X(u)\|^4 + 3^{4c} \|X(u)\|^{4c+4}) \middle| \mathcal{F}_{t_n} \right]}.$$

A similar approach for R_g using the global Lipschitz condition (4) completes Part (ii).

Part (iii) follows from the construction of \bar{K}_1 and \bar{K}_2 as follows. An application of Cauchy Schwarz and (5) in the statement of Lemma 1 gives that there exists $K_1 < \infty$, independent of h_{n+1} , such that

$$\mathbb{E} [\bar{K}_1] = \mathbb{E} \left[\frac{2}{3} \sqrt{\bar{M}_n} \sqrt{\bar{L}_n} \right] \leq \frac{2}{3} \sqrt{\mathbb{E} [\bar{M}_n]} \sqrt{\mathbb{E} [\bar{L}_n]} =: K_1.$$

A similar argument using Jensen's inequality shows that there exists $K_2 < \infty$, independent of h_{n+1} , such that $\mathbb{E} [\bar{K}_2] \leq K_2$.

Finally, for Part (iv), define the a.s. finite and \mathcal{F}_{t_n} -measurable random variable

$$P(\|X(t_n)\|) := R_1 + 2R_2 \|X(t_n)\|^2 c_1^2 \left(1 + 2\|X(t_n)\|^{c+1} + \|X(t_n)\|^{2(c+1)} \right).$$

Then, by Cauchy-Schwarz and (5) in the statement of Lemma 1, we have that there exists $K_3 < \infty$, independent of h_{n+1} , such that

$$\mathbb{E} [\bar{K}_1 P(\|X(t_n)\|)] = \mathbb{E} \left[\sqrt{\bar{M}_n} \sqrt{\bar{L}_n} P(\|X(t_n)\|)^2 \right] \leq \mathbb{E} \left[\sqrt{\bar{M}_n} \sqrt{\bar{L}_n^*} \right] = K_3,$$

where, by (26), we have

$$\begin{aligned} \bar{L}_n^* = 4\mathbb{E} \left[c_1^2 \sup_{u \in [0, T]} ((1 + \|X(u)\|^{2c+2}) P(\|X(u)\|^2) \middle| \mathcal{F}_{t_n} \right] \\ + 2\kappa^2 \mathbb{E} \left[\sup_{u \in [0, T]} (\|X(u)\|^2 P(\|X(u)\|^2) \middle| \mathcal{F}_{t_n} \right]. \end{aligned}$$

This completes the proof. \square

Proof of Theorem 12. By Theorem 6 it is sufficient to consider only the event that $h_{\min} < h_n < h_{\max}$ for all $n = 0, \dots, N-1$. Define the error sequence $\{E_n\}_{n \in \mathbb{N}}$ by

$$\begin{aligned} E_{n+1} &:= Y_{n+1} - X(t_{n+1}) \\ &= Y_n - X(t_n) + \int_{t_n}^{t_{n+1}} [f(Y_n) - f(X(s))] ds + \int_{t_n}^{t_{n+1}} [g(Y_n) - g(X(s))] dW(s). \end{aligned}$$

Expand f and g as Taylor series around $X(t_n)$ over the interval of integration. As in Lemma 14 we get

$$\begin{aligned} E_{n+1} = E_n + \int_{t_n}^{t_{n+1}} [f(Y_n) - f(X(t_n))] ds + \int_{t_n}^{t_{n+1}} [g(Y_n) - g(X(t_n))] dW(s) \\ + \underbrace{\int_{t_n}^{t_{n+1}} R_f(s, t_n, X(t_n)) ds}_{:= \tilde{R}_f(t_n, X(t_n))} + \underbrace{\int_{t_n}^{t_{n+1}} R_g(s, t_n, X(t_n)) dW(s)}_{:= \tilde{R}_g(t_n, X(t_n))} \end{aligned}$$

which may be rewritten using the notation $\triangle W_{n+1} = W(t_{n+1}) - W(t_n)$ as

$$\begin{aligned} E_{n+1} = E_n + h_{n+1} [f(Y_n) - f(X(t_n))] + \triangle W_{n+1} [g(Y_n) - g(X(t_n))] \\ + \tilde{R}_f(t_n, X(t_n)) + \tilde{R}_g(t_n, X(t_n)). \end{aligned}$$

Next we develop appropriate bounds on

$$(28) \quad \mathbb{E} [\|E_{n+1}\|^2 | \mathcal{F}_{t_n}] = \mathbb{E} [\langle E_{n+1}, E_{n+1} \rangle | \mathcal{F}_{t_n}].$$

Note that

$$\begin{aligned} \|E_{n+1}\|^2 &= \langle E_n, E_{n+1} \rangle + \underbrace{h_{n+1} \langle f(Y_n) - f(X(t_n)), E_{n+1} \rangle}_{:= A_n} \\ &+ \underbrace{\langle \triangle W_{n+1} [g(Y_n) - g(X(t_n))], E_{n+1} \rangle}_{:= B_n} + \underbrace{\langle \tilde{R}_f(t_n, X(t_n)) + \tilde{R}_g(t_n, X(t_n)), E_{n+1} \rangle}_{:= C_n}. \end{aligned}$$

Then, since $\langle E_n, E_{n+1} \rangle \leq \frac{1}{2}(\|E_n\|^2 + \|E_{n+1}\|^2)$, we have $\|E_{n+1}\|^2 = \|E_n\|^2 + 2A_n +$

$2B_n + 2C_n$. Next we omit the arguments from \tilde{R}_f , \tilde{R}_g and write

$$\begin{aligned}
A_n &= h_{n+1} \langle f(Y_n) - f(X(t_n)), E_n \rangle + h_{n+1}^2 \|f(Y_n) - f(X(t_n))\|^2 \\
&\quad + h_{n+1} \langle f(Y_n) - f(X(t_n)), \Delta W_{n+1}[g(Y_n) - g(X(t_n))] \rangle \\
&\quad + h_{n+1} \langle f(Y_n) - f(X(t_n)), \tilde{R}_f + \tilde{R}_g \rangle; \\
B_n &= \langle \Delta W_{n+1}[g(Y_n) - g(X(t_n))], E_n \rangle + \|\Delta W_{n+1}[g(Y_n) - g(X(t_n))]\|^2 \\
&\quad + h_{n+1} \langle \Delta W_{n+1}[g(Y_n) - g(X(t_n))], f(Y_n) - f(X(t_n)) \rangle \\
&\quad + \langle \Delta W_{n+1}[g(Y_n) - g(X(t_n))], \tilde{R}_f + \tilde{R}_g \rangle; \\
C_n &= \langle \tilde{R}_f + \tilde{R}_g, E_n \rangle + \|\tilde{R}_f + \tilde{R}_g\|^2 \\
&\quad + h_{n+1} \langle \tilde{R}_f + \tilde{R}_g, f(Y_n) - f(X(t_n)) \rangle \\
&\quad + \langle \Delta W_{n+1}[g(Y_n) - g(X(t_n))], \tilde{R}_f + \tilde{R}_g \rangle.
\end{aligned}$$

By [Remark 9](#), and applying the Lipschitz bounds [\(3\)](#) and [\(4\)](#), we may now estimate [\(28\)](#) as

$$\begin{aligned}
&\mathbb{E} [\|E_{n+1}\|^2 | \mathcal{F}_{t_n}] \\
&\leq \|E_n\|^2 + h_{n+1}(2\alpha + 2\kappa^2) \|E_n\|^2 + 2h_{n+1}^2 \|f(Y_n) - f(X(t_n))\|^2 \\
&\quad + \underbrace{4h_{n+1} \mathbb{E} [\langle f(Y_n) - f(X(t_n)), \tilde{R}_f + \tilde{R}_g \rangle | \mathcal{F}_{t_n}]}_{:= \bar{A}_n} \\
&\quad + \underbrace{4\mathbb{E} [\langle \Delta W_{n+1}[g(Y_n) - g(X(t_n))], \tilde{R}_f + \tilde{R}_g \rangle | \mathcal{F}_{t_n}]}_{:= \bar{B}_n} \\
&\quad + \underbrace{2\mathbb{E} [\langle \tilde{R}_f + \tilde{R}_g, E_n \rangle | \mathcal{F}_{t_n}]}_{:= \bar{C}_n} + \underbrace{2\mathbb{E} [\|\tilde{R}_f + \tilde{R}_g\|^2 | \mathcal{F}_{t_n}]}_{:= \bar{D}_n}, \quad a.s.
\end{aligned}$$

Since $\{t_n\}_{n \in \mathbb{N}}$ arises from an admissible timestepping strategy, we can use [\(20\)](#) along with the bound on [\(6\)](#) on f to get

$$\begin{aligned}
&h_{n+1}^2 \|f(Y_n) - f(X(t_n))\|^2 \\
&\leq 2h_{n+1}^2 \|f(Y_n)\|^2 + 2h_{n+1}^2 \|f(X(t_n))\|^2 \\
&\leq 2h_{n+1}^2 R_2 \|Y_n\|^2 + 2h_{n+1}^2 R_1 + 2h_{n+1}^2 \|f(X(t_n))\|^2 \\
&\leq 4h_{n+1}^2 R_2 \|E_n\|^2 + 4h_{n+1}^2 R_2 \|X(t_n)\|^2 + 2h_{n+1}^2 R_1 + 2h_{n+1}^2 \|f(X(t_n))\|^2 \\
&\leq 4h_{n+1}^2 R_2 \|E_n\|^2 + 2h_{n+1}^2 R_1 \\
(29) \quad &+ 4h_{n+1}^2 R_2 \|X(t_n)\|^2 + 2c_1^2 h_{n+1}^2 \left(1 + 2\|X(t_n)\|^{c+1} + \|X(t_n)\|^{2(c+1)}\right).
\end{aligned}$$

Now we can write

$$\begin{aligned}
(30) \quad \mathbb{E} [\|E_{n+1}\|^2 | \mathcal{F}_{t_n}] - \|E_n\|^2 &\leq h_{n+1}(2\alpha + 2\kappa^2 + 8R_2) \|E_n\|^2 \\
&\quad + 4h_{n+1}^2 \left[R_1 + 2R_2 \|X(t_n)\|^2 + c_1^2 \left(1 + 2\|X(t_n)\|^{c+1} + \|X(t_n)\|^{2(c+1)}\right) \right] \\
&\quad + \bar{A}_n + \bar{B}_n + \bar{C}_n + \bar{D}_n, \quad a.s.
\end{aligned}$$

Next we must consider the terms \bar{A}_n , \bar{B}_n , \bar{C}_n , and \bar{D}_n . After an application of the triangle inequality, it immediately follows from Part (ii) of [Lemma 14](#) that

$$\bar{D}_n = 2\mathbb{E} [\|\tilde{R}_f + \tilde{R}_g\|^2 | \mathcal{F}_{t_n}] \leq 8\bar{K}_2 h_{n+1}^2, \quad a.s.$$

This estimate, along with the conditional second moment of ΔW_{n+1} provided in [Remark 9](#), and additionally applying two variants of the Cauchy-Schwarz inequality, first to the inner product and second to the conditional expectation, gives us

$$\begin{aligned}
\bar{B}_n &= 4\mathbb{E} \left[\langle \Delta W_{n+1} [g(Y_n) - g(X(t_n))], \tilde{R}_f + \tilde{R}_g \rangle | \mathcal{F}_{t_n} \right] \\
&\leq \kappa \|E_n\| \mathbb{E} \left[\langle \Delta W_{n+1}, \tilde{R}_f + \tilde{R}_g \rangle | \mathcal{F}_{t_n} \right] \\
&\leq \kappa \|E_n\| \mathbb{E} \left[\|\Delta W_{n+1}\| \|\tilde{R}_f + \tilde{R}_g\| | \mathcal{F}_{t_n} \right] \\
&\leq \kappa \|E_n\| \sqrt{\mathbb{E} [\|\Delta W_{n+1}\|^2 | \mathcal{F}_{t_n}]} \sqrt{\mathbb{E} [\|\tilde{R}_f + \tilde{R}_g\|^2 | \mathcal{F}_{t_n}]} \\
&\leq 2\kappa \sqrt{\bar{K}_2} \|E_n\| h_{n+1}^{3/2} \\
&\leq \frac{1}{2} \|E_n\|^2 h_{n+1} + \kappa^2 \bar{K}_2 h_{n+1}^2, \quad a.s.
\end{aligned}$$

Part (i) of [Lemma 14](#) yields

$$\begin{aligned}
\bar{C}_n &= 2\mathbb{E} \left[\langle \tilde{R}_f + \tilde{R}_g, E_n \rangle | \mathcal{F}_{t_n} \right] \\
&\leq 2\mathbb{E} \left[\|\tilde{R}_f\| \|E_n\| | \mathcal{F}_{t_n} \right] + 2\mathbb{E} \left[\|\tilde{R}_g\| \|E_n\| | \mathcal{F}_{t_n} \right] \\
&\leq 4\bar{K}_1 \|E_n\| h_{n+1}^{3/2} \leq 2\bar{K}_1 h_{n+1} \|E_n\|^2 + 2\bar{K}_1 h_{n+1}^2, \quad a.s.
\end{aligned}$$

Finally,

$$\begin{aligned}
\bar{A}_n &= 4h_{n+1} \mathbb{E} \left[\langle f(Y_n) - f(X(t_n)), \tilde{R}_f + \tilde{R}_g \rangle | \mathcal{F}_{t_n} \right] \\
&= 4h_{n+1} \mathbb{E} \left[\langle f(Y_n) - f(X(t_n)), \tilde{R}_f \rangle | \mathcal{F}_{t_n} \right] + 4h_{n+1} \mathbb{E} \left[\langle f(Y_n) - f(X(t_n)), \tilde{R}_g \rangle | \mathcal{F}_{t_n} \right].
\end{aligned}$$

Moreover we have

$$\begin{aligned}
\mathbb{E} \left[\langle f(Y_n) - f(X(t_n)), \tilde{R}_f \rangle | \mathcal{F}_{t_n} \right] &\leq \mathbb{E} \left[\|f(Y_n) - f(X(t_n))\| \|\tilde{R}_f\| | \mathcal{F}_{t_n} \right] \\
&= \|f(Y_n) - f(X(t_n))\| \mathbb{E} \left[\|\tilde{R}_f\| | \mathcal{F}_{t_n} \right] \quad a.s.
\end{aligned}$$

A similar bound holds for $\mathbb{E} \left[\langle f(Y_n) - f(X(t_n)), \tilde{R}_g \rangle | \mathcal{F}_{t_n} \right]$, and therefore, by Part (i) of [Lemma 14](#),

$$\begin{aligned}
\bar{A}_n &\leq 8\|f(Y_n) - f(X(t_n))\| \bar{K}_1 h_{n+1}^{5/2} \\
&\leq 4\bar{K}_1 h_{n+1}^2 + 4\bar{K}_1 \|f(Y_n) - f(X(t_n))\|^2 h_{n+1}^3, \quad a.s.
\end{aligned}$$

Applying these bounds to (30), along with (29) and noting that $h_{\max} \leq 1$, yields

$$\begin{aligned}
(31) \quad \mathbb{E} [\|E_{n+1}\|^2 | \mathcal{F}_{t_n}] - \|E_n\|^2 &\leq h_{n+1} \Gamma_2 \|E_n\|^2 \\
&\quad + [6\bar{K}_1 + (8 + \kappa^2)\bar{K}_2 + 4(1 + \bar{K}_1) [R_1 + 2R_2 \|X(t_n)\|^2 \\
&\quad \quad + c_1^2 (1 + 2\|X(t_n)\|^{c+1} + \|X(t_n)\|^{2(c+1)})]] h_{n+1}^2, \quad a.s.
\end{aligned}$$

where, recalling K_1 as defined in Part (iii) of the statement of [Lemma 14](#),

$$\Gamma_2 := 2(\alpha + \kappa^2) + 1/2 + 2K_1 + 24R_2.$$

Summing both sides of (31) over n from 0 to $N - 1$ and taking expectations yields

$$(32) \quad \mathbb{E}[\|E_N\|^2] \leq \Gamma_1 Th_{\max} + \Gamma_2 h_{\max} \sum_{n=0}^{N-1} \mathbb{E}[\|E_n\|^2],$$

where, recalling K_2 and K_3 as defined in Parts (iii) and (iv) of the statement of [Lemma 14](#), we have defined the constant Γ_1 as

$$\begin{aligned} \Gamma_1 := & 6K_1 + (8 + \kappa^2)K_2 + 4 \left[R_1 + 2R_2 \mathbb{E} \left[\sup_{u \in [0, T]} \|X(u)\|^2 \right] \right. \\ & \left. + c_1^2 \left(1 + 2\mathbb{E} \left[\sup_{u \in [0, T]} \|X(u)\|^{c+1} \right] + \mathbb{E} \left[\sup_{u \in [0, T]} \|X(u)\|^{2(c+1)} \right] \right) \right] + 4K_3. \end{aligned}$$

The discrete Gronwall inequality (see for example [\[23\]](#)), [\(11\)](#), and the fact that $Nh_{\min} \leq T$, may now be applied to [\(32\)](#):

$$\begin{aligned} \mathbb{E}[\|E_N\|^2] & \leq \Gamma_1 Th_{\max} \exp \{Nh_{\max} \Gamma_2\} \\ & = \Gamma_1 Th_{\max} \exp \{\rho Nh_{\min} \Gamma_2\} \\ & \leq \Gamma_1 Th_{\max} \exp \{\rho T \Gamma_2\}, \end{aligned}$$

which gives the statement of the theorem. \square

5. Conclusions and future work. We introduced a class of adaptive timestepping strategies for SDEs with non-Lipschitz drift coefficients and proved strong convergence without the need to prove additional moment bounds on the numerical method.

Our numerical results on the stochastic Van der Pol equation indicate that adaptive timestepping may lead to dynamically more accurate solutions than those from a fixed step tamed scheme where the drift is perturbed, this was not only true for the two adaptive schemes we presented here. From the suite of problems we examined the method ALD seems to lead to a smaller variance in the timestep selection. We also saw from the numerical experiments that the parameter ρ required in the analysis is not a restriction. Adaptive timestepping strategies are readily applicable to large scale systems, such as the Allen-Cahn SPDE. We also saw that when applied in a MLMC context adaptivity can lead to more efficient computation. It has already been noted by a number of authors [\[3, 17, 22\]](#) that adaptivity may be useful for Langevin sampling dynamics and our analysis offers techniques suitable for equations with non-Lipschitz drift terms that may arise, for example, in image processing. We also note that this approach could be combined with error control timestepping strategies.

Possible future work includes extending the analysis to include to SDEs with non-Lipschitz diffusion coefficients, to SDEs with Lévy noise, to SPDEs and to other forms of explicit methods.

6. Acknowledgement. The authors thank Prof. Alexandra Rodkina (UWI) for her feedback on an earlier draft.

- [1] J. A. D. Appleby, C. Kelly, and A. Rodkina. On the Use of Adaptive Meshes to Counter Overshoot in Solutions of Discretised Nonlinear Stochastic Differential Equations. *International Journal of Difference Equations*, 5(2):129–148, 2010.
- [2] J.A.D. Appleby, C. Kelly, X. Mao, and A. Rodkina. On the local dynamics of polynomial difference equations with fading stochastic perturbations. *Dyn. Contin. Discrete Impuls. Syst. Ser. A Math. Anal.*, 17(3):401–430, 2010.
- [3] A. Beskos, N. Pillai, G. Roberts, J-M. Sanz-Serna, and A. Stuart. Optimal tuning of the hybrid Monte Carlo algorithm. *Bernoulli*, 19(5A):1501–1534, 11 2013.
- [4] W-J. Beyn, E. Isaak, and R. Kruse. Stochastic C-stability and B-consistency of explicit and implicit Euler-type schemes. *Journal of Scientific Computing*, 67(3):955–987, 2016.
- [5] P. M. Burrage, R. Herdiana, and K. Burrage. Adaptive stepsize based on control theory for stochastic differential equations. *Journal of Computational and Applied Mathematics*, 171(1-2):317–336, 2004.
- [6] K. Dareiotis, C. Kumar, and S. Sabanis. On tamed Euler approximations of SDEs driven by Lévy noise with applications to delay equations. *SIAM J. Numer. Anal.*, 54(3):1840–1872, 2016.
- [7] W. Fang and M. Giles. Adaptive Euler-Maruyama method for SDEs with non-globally Lipschitz drift: Part I, finite time interval. *arXiv:1609.08101*, September 2016.
- [8] M. B. Giles. Multilevel Monte Carlo methods. *Acta Numerica*, 24:259–328, 2015.
- [9] I. Gyöngy, S. Sabanis, and D. Šiška. Convergence of tamed Euler schemes for a class of stochastic evolution equations. *Stoch. Partial Differ. Equ. Anal. Comput.*, 4(2):225–245, 2016.
- [10] D. J. Higham, X. Mao, and A. M. Stuart. Strong convergence of Euler-type methods for nonlinear stochastic differential equations. *SIAM J. Numer. Anal.*, 40(3):1041–1063, 2002.
- [11] H. Hoel, E. von Schwerin, A. Szepessy, and R. Tempone. Implementation and analysis of an adaptive multilevel Monte Carlo algorithm. *Monte Carlo Methods appl.*, 20:1–41, 2014.
- [12] M. Hutzenthaler and A. Jentzen. Numerical approximations of stochastic differential equations with non-globally Lipschitz continuous coefficients. *Mem. Amer. Math. Soc.*, 236(1112):v+99, 2015.
- [13] M. Hutzenthaler, A. Jentzen, and P. E. Kloeden. Strong and weak divergence in finite time of Euler’s method for stochastic differential equations with non-globally Lipschitz continuous coefficients. *Proc. R. Soc. Lond. Ser. A Math. Phys. Eng. Sci.*, 467(2130):1563–1576, 2011.
- [14] M. Hutzenthaler, A. Jentzen, and P. E. Kloeden. Strong convergence of an explicit numerical method for SDEs with nonglobally Lipschitz continuous coefficients. *Ann. Appl. Probab.*, 22(4):1611–1641, 2012.
- [15] S. Ilie, K. R. Jackson, and W. H. Enright. Adaptive time-stepping for the strong numerical solution of stochastic differential equations. *Numer. Algorithms*, 68(4):791–812, 2015.
- [16] P.E. Kloeden and E. Platen. *Numerical Solution of Stochastic Differential Equations*. Stochastic Modelling and Applied Probability. Springer Berlin Heidelberg, 2011.
- [17] H. Lamba, J. C. Mattingly, and A. M. Stuart. An adaptive Euler-Maruyama scheme for SDEs: convergence and stability. *IMA J. Numer. Anal.*, 27(3):479–506, 2007.
- [18] G. J. Lord, C. E. Powell, and T. Shardlow. *An introduction to computational stochastic PDEs*. Cambridge Texts in Applied Mathematics. Cambridge University Press, New York, 2014.
- [19] X. Mao. Convergence rates of the truncated Euler-Maruyama method for stochastic differential equations. *J. Comput. Appl. Math.*, 296:362–375, 2016.
- [20] S. Sabanis. A note on tamed Euler approximations. *Electron. Commun. Probab.*, 18:no. 47, 10, 2013.
- [21] T. Shardlow and P. Taylor. On the pathwise approximation of stochastic differential equations. *arXiv*, 2015. 1409.2362v3.
- [22] V. Sotiropoulos and Y. N. Kaznessis. An adaptive time step scheme for a system of stochastic differential equations with multiple multiplicative noise: Chemical Langevin equation, a proof of concept. *Journal of Chemical Physics*, 2008.
- [23] A. M. Stuart and A. R. Humphries. *Dynamical Systems and Numerical Analysis*. CUP, 1996.
- [24] M. V. Tretyakov and Z. Zhang. A fundamental mean-square convergence theorem for SDEs with locally Lipschitz coefficients and its applications. *SIAM J. Numer. Anal.*, 51(6):3135–3162, 2013.
- [25] X. Wang and S. Gan. The tamed Milstein method for commutative stochastic differential equations with non-globally Lipschitz continuous coefficients. *Journal of Difference Equations and Applications*, 19(3):466–490, 2013.